

Green Synthesis of α -Fe₂O₃ Nanoparticles Using Pistachio Leaf Extract Influenced Seed Germination and Seedling Growth of Tomatos

Majd Abusalem¹, Akl Awwad², Jamal Ayad^{1*}, Azmi Abu Rayyan¹

¹University of Jordan, Department of Horticulture and Crop Science, Faculty of Agriculture, Jordan

²Royal Scientific Society, Department of Nanomaterials, Jordan

Received 7 April 2019; Accepted 19 May 2019

Abstract

The objective of this study is to assess the effects of the green synthesis of Hematite (α -Fe₂O₃) nanoparticles derived from pistachio (*Pistacia vera* L) leaves on seed germination and seedling growth of tomato (*Lycopersicon esculentum* L.). Hematite (α -Fe₂O₃) nanoparticles were synthesized using the pistachio leaves aqueous extract at ambient temperature. X-ray diffraction characterized the final product as crystalline α -Fe₂O₃ with the size of 40 nm. The seeds were then treated with different concentrations of α -Fe₂O₃ (10, 40, 80, 100 and 200 ppm). The transmission electron microscopy results reveal the presence of a network of randomly-oriented α -Fe₂O₃ spherical nanoparticles with an average size of 40 nm. The green synthesized α -Fe₂O₃ nanoparticles significantly improved seed vigor index, shoot length, fresh and dry weight of the tomato seedlings. Interestingly, lower concentration (10 ppm) of α -Fe₂O₃ nanoparticles improved the vigor index by 24 %, shoot length by 48.6 %, seedling fresh weight by 41 %, and seedling dry weight by 135 % compared to control ($p < 0.025$, $p < 0.001$, $p < 0.005$ and $p < 0.01$; respectively). Overall, the results of the current study show that the green synthesis of the nanoparticles from the pistachio leaves' extract holds promise in that the synthesized nanoparticles can enhance seed germination and seedling vigor of tomatos.

© 2019 Jordan Journal of Earth and Environmental Sciences. All rights reserved

Keywords: Hematite nanoparticles, Pistachio vera, green synthesis, *Lycopersicon esculentum*.

1. Introduction

Iron-oxide nanoparticles have drawn the attention recently because they can improve the ability of plants to absorb iron oxides. Those nanoparticles (1–100 nm size) have distinctive physio-chemical characteristics that deliver iron oxides to plants efficiently (Ramimoghadam et al., 2014). Hematite (α -Fe₂O₃), the firmly-stable form of iron-oxide nanoparticles normally exists in rhombohedral crystal units and has an important role in research and technology (Kolen'ko et al., 2014). For example, it can be utilized as a startup for the synthesis of magnetite and maghemite. Moreover, the α -Fe₂O₃ nanoparticles have been widely utilized in soil decontamination, water quality, engineering (Dong et al., 2016), and agriculture (Asoufi et al., 2018).

Iron-oxide nanoparticles can be synthesized using several chemical and physical procedures. However, those procedures require costly and highly complicated equipments, tremendous pressure and temperature, additional purification procedures that could produce harmful derivatives and byproducts. Conversely, green synthesis has been suggested as an alternative because the manufacturing of metal-oxide nanoparticles using this approach is environmentally friendly and safe (Ahmmad et al., 2013).

Most of nanotechnology researches are concerned with adopting green synthesis to cope with the limitations of other common methods (Seabra et al., 2013). In general, plant tissue (Shameli et al., 2012), plant extracts (Parsons et

al., 2007) and other parts of living plants (Jain et al., 2005) are used to synthesize nano-sized materials. This approach is environmentally safe, free from chemical contamination, less expensive, nontoxic, and can be utilized in biological applications (Groiss et al., 2017) in comparison to the commonplace chemical method where many noxious and permanent chemical substances are applied (Nadagouda et al., 2009). From the environment awareness point of view, green approaches are regarded as successful methods for producing metal nanoparticles. Also, when using the green method for Hematite production, it is not essential for the chemical to be stabilized and reduced, in addition to the fact that its manufacturing can be done under normal circumstances including temperature and pressure (Ren et al., 2017).

Using plant extracts in hematite production is simple, and is of a low cost. Moreover it entails utilizing bio-products which renders it acceptable as an eco-friendly method. Hematite nanoparticles have been synthesized using various plant species (Jagathesan and Rajiv, 2018), such as, *Camellia sinensis* (Hoag et al., 2009; Ahmmad et al., 2013), *Citrus reticulatum* peels (Ali et al., 2017), *Cyprus rotundus* L. (Basavegowda et al., 2017), Roman nettle (Badni et al., 2016), and *Eucalyptus globules* (Madhavi et al., 2013). Limited research studies have documented the effects of iron-oxide nanoparticle on plants during germination (Pariona et al., 2017). Iron-oxide nanoparticles were found to increase germination in Chinese mung beans (Ren et al.,

* Corresponding author e-mail: ayadj@ju.edu.jo

2011), corn (Li et al., 2016) and oaks (Pariona et al., 2017). However, to the researchers' knowledge, no study has yet assessed the effects of the green-synthesis of hematite (α -Fe₂O₃) nanoparticles on seed germination and seedling growth of tomato plants. The present study was designed to synthesize hematite (α -Fe₂O₃) nanoparticles with a novel, rapid, clean, non-toxic, and environmentally acceptable green route. The approach of this study uses the iron salt precursor in the presence of pistachio leaves' aqueous extract via a single step reaction. This environmentally-friendly product (α -Fe₂O₃) was then used to investigate this research's objectives which hypothesized that the synthesized hematite (α -Fe₂O₃) nanoparticles can improve germination and growth parameters of tomato seeds.

2. Materials and Methods

2.1 Preparation of Pistachio Aqueous Extract

Mature Pistachio Leaves were collected from the local garden of the Royal Scientific Society, Jordan. The fresh green leaves were washed, cleaned and air-dried for seven days at room temperature (28 °C/ 15 °C, 41% relative humidity). Twenty grams of leaves were placed into 500 ml of deionized water and heated at 90°C for twenty minutes. The aqueous extract was cooled down and filtered through Whatman filter paper (porosity 25 μm) to remove the solid particles. Afterwards, the extract was stored in a glass bottle with a tight cover at room temperature to be used later for the synthesis of iron-oxides nanoparticles.

2.2 Preparation of Hematite (α -Fe₂O₃) Nanoparticles

The preparation of the α -Fe₂O₃ nanoparticles was conducted in the Royal Scientific Society Labs, Amman, Jordan. Four grams of iron nitrate nonahydrate (Fe (NO₃)₃·9H₂O; Sigma-Aldrich), used as a precursor for the Fe²⁺ ions, were dissolved in 400ml of de-ionized water under magnetic stirring at room temperature (27°C). Next, the prepared aqueous solution of the pistachio leaf extract (~ 100 ml) was progressively added to the iron-nitrate solution. The yellow color of the iron nitrate nonahydrate was changed to dark-red-brown indicating the formation of iron hydroxide. Then, a 5 % NaOH solution (99.5 %, BBC chemicals for lab) was added progressively in anticipation for the pH to reach the alkaline status (pH~10–12) and to act as a precipitation agent. The suspended red-brown particle solution was left under magnetic stirring for two hours. The suspension was purified with sterile de-ionized water three times. To get pure α -Fe₂O₃ nanoparticles the precipitate was dried under vacuum, and was heated up to 550°C for two hours. The steps are demonstrated in equations 1-3 and in Figure 1. The prepared samples of the iron oxides were used for further characterization and for the nanoparticle synthesis.

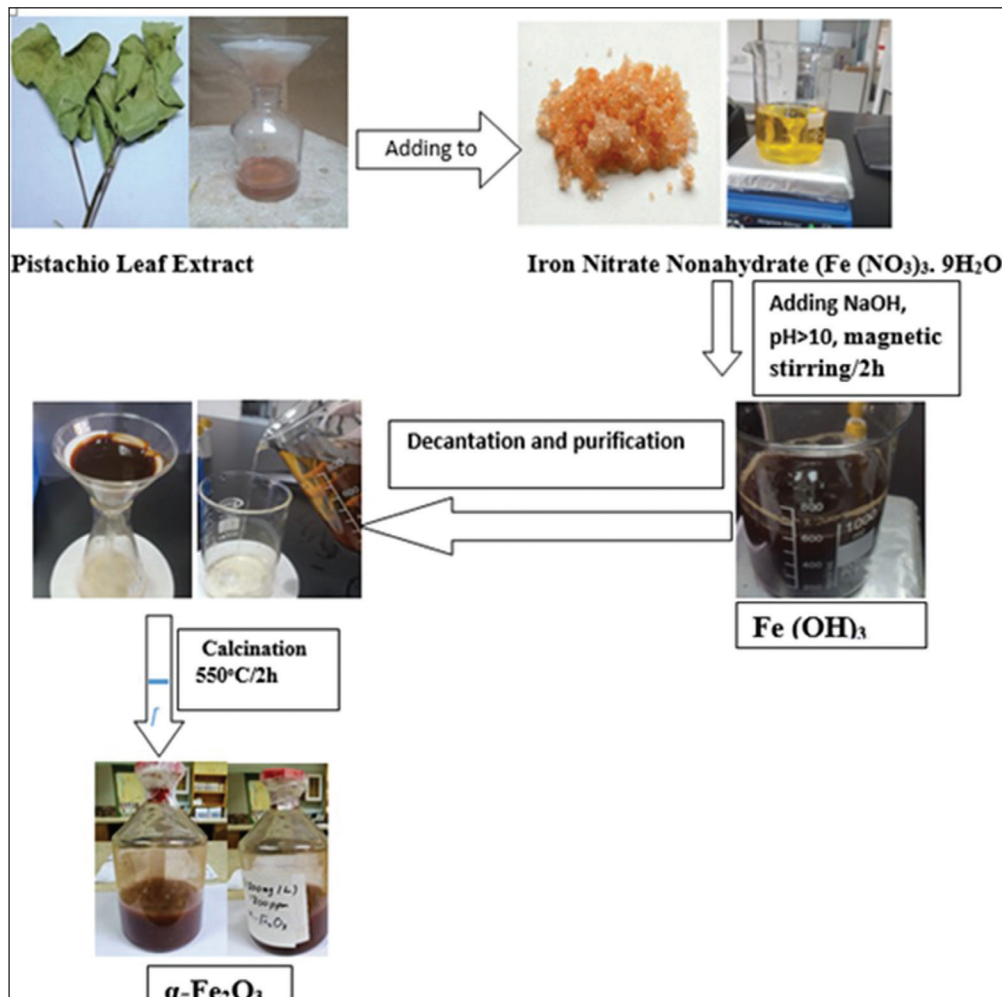
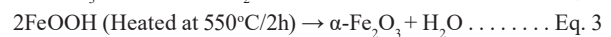


Figure 1. Schematic illustration of the green synthesis of hematite (α -Fe₂O₃) nanoparticles using *P. vera* leaves as aqueous extract.

2.3 Characterization of Hematite ($\alpha\text{-Fe}_2\text{O}_3$) Nanoparticles

The Fourier transform infrared spectrophotometer (FT-IR, Shimadzu, IR-Prestige-21) was used to identify possible functional groups such as (NH, C=O carboxylic acid, C-N, OH phenols, OH alcohol, OH water) in the plant extract and in the synthesized hematite ($\alpha\text{-Fe}_2\text{O}_3$) nanoparticles. The sample was scanned by X-ray diffraction (XRD-6000, Shimadzu) ($\lambda=1.5405\text{nm}$) within the 2θ range of ($3^\circ - 80^\circ$) by applying the Debye–Scherer’s equation (Awwad and Salem, 2012):

$$D = 0.9\lambda/\beta\cos\theta \dots \dots \dots \text{Equation 4}$$

where D is the crystallite size, λ is the X-ray wavelength, β is the full width at half maximum of the diffraction peak, and θ is the diffraction (Bragg) angle of the XRD spectra. The ultraviolet visible spectroscopy (SPUV-26, Sco-tech) was used to prove the forming and exact structure of the hematite ($\alpha\text{-Fe}_2\text{O}_3$) nanoparticles in colloidal media. The transmission electron microscopy spectroscopy (TEM) (JEM-2100, JEOL Co.) was conducted to figure out the morphology, size, and distribution of the synthesized hematite ($\alpha\text{-Fe}_2\text{O}_3$) nanoparticles.

2.4 Effect of Hematite ($\alpha\text{-Fe}_2\text{O}_3$) Nanoparticles on Seed Germination of Tomatos

This experiment was carried out over the period from October 16-28, 2018 under laboratory conditions at the University of Jordan, Amman, Jordan. The impact of various concentrations of hematite nanoparticles on the germination of tomato seeds (*Lycopersicon esculentum* L. var Newton). The seeds were surface-sterilized with 50 % ethanol for one minute, and were rinsed once for one minute by 10 % commercial bleach (Sodium hypochlorite). Finally, they were washed extensively with sterilized water. One-hundred and eighty tomato seeds were grown in plastic trays (30cm x 10 cm). Thirty seeds per tray (three replicates and ten seeds per replicate) were used. Each tray was considered as an experimental unit. The seeds were wetted with 5 ml of six levels of hematite nanoparticles as follows: 0 (control), 10, 40, 80, 100, and 200 ppm. The trays were then covered tightly with transparent lids. The germination tests were performed according to the rules issued by the International Seed Testing Association (ISTA, 2009). The germination counts and seedling evaluations were performed daily for ten days. Seeds were considered germinated when the radical was emerged to a length of 2 mm. At the end of the experiment, the root and shoot fresh weights were measured using a four-digit balance. Germination indices such as germination percentage (G %), germination rate (GR) and Vigor index (VI) were calculated using the following equations:

$$\text{Germination percent (G \%)} = (Gf/N) \times 100 \dots \dots \text{Equation 5}$$

Where Gf is the total number of germinated seeds at the end of experiment, and N is the total number of seeds used in the test.

$$\text{Germination rate (GR)} = (a/1) + (b-a/2) + (c-b/3) + \dots + (nn-1/N) \dots \dots \text{Equation 6}$$

Where a, b, c, and n are the numbers of the germinated seeds after 1, 2, 3, and N days from the start of imbibition.

$$\text{Vigor index (VI)} = SL \times G \% \dots \dots \dots \text{Equation 7}$$

Where SL is the seedling length (root length + shoot

length), and G % is the germination percentage.

Root samples taken from the germinated seeds were scanned using a root scanner (Regent STD 1600+, Regent Instruments, QC, Canada). Root length and diameter and shoot length were measured using image analysis software, WinRhizo Pro (Regent Instruments). The root samples were then dried at 70°C for dry weight determination (Ayad, et al., 2010).

2.5 Statistical Analysis

Statistical analyses were conducted using SAS (version 9.4, SAS institute, Cary, NC). Significance was defined at $\alpha = 0.05$. The experiment was allocated using a complete randomized design (CRD) with three replications (ten subsamples) and six FeNPs concentrations. Data for each experimental unit were averaged and statistically analyzed. One-way ANOVA using General Linear Model (proc GLM) with the Fisher’s LSD mean separation test were used to analyze the shoot length, root length, fresh weight, dry weight, germination percentage (G%), germination rate (GR), and vigor index (VI).

3. Results and Discussion

3.1 FT-IR Analysis

The FT-IR spectra of the *P. vera* aqueous leaf extract showed a distinctive broad and a peak ($3433\text{-}3352\text{ cm}^{-1}$). This was attributed to the N-H stretching and bending vibration of amine group NH_2 and hydroxyl O-H (Figure 2). The overlapping of the stretching vibration is attributed to the water and the *P. vera* aqueous leaf extract molecules. The peaks at 2924 cm^{-1} and 2850 cm^{-1} are attributed to the stretching vibrations of $-\text{CH}_2$ and $-\text{CH}_3$ functional groups. The sharp band at 1724 cm^{-1} was a result of the amid carbonyl group as amide I and amide II, which appeared because of C=O and NH stretching vibrations in the amide linkage of the protein. The peaks at $1604, 1531, 1450, 1334,$ and 1207 cm^{-1} can be attributed to the C-O group of polyols. The peaks around 1099 cm^{-1} might be ascribed to the C-N stretching vibrations of the aliphatic amines. These results agreed with the findings reported by Salem et al. (2013) upon the investigation of the *P. vera* aqueous leaves’ extract FT-IR

The synthesized hematite ($\alpha\text{-Fe}_2\text{O}_3$) nanoparticles are characterized by FT-IR spectra. This is normally to determine the probable biological molecules behind the oxidation of Fe^{3+} , capping, and the stabilization of nanoparticles. Figure 3 shows that the peaks at 3691 cm^{-1} and 3401 cm^{-1} are attributed to the O-H stretching -NH stretching and the bending vibration of amine NH_2 group in the *P. vera* leaf extract, and the overlap of the stretching vibration of O-H. The peak at 1358 cm^{-1} could be attributed to the asymmetric and symmetric stretching vibration of COO^- . The presence of hematite ($\alpha\text{-Fe}_2\text{O}_3$) nanoparticles was identified by the presence of two absorption bands approximately at 536 cm^{-1} and 455 cm^{-1} , which correspond to the Fe-O stretching bands of the bulk hematite (Fe_2O_3). These results indicate that the COO^- groups were attached to the hematite particle surface. Generally, the observation indorses the existence of protein in the *P. vera* aqueous leaf extract, which acts as an oxidizing and capping agent and as a stabilizer for the hematite nanoparticles.

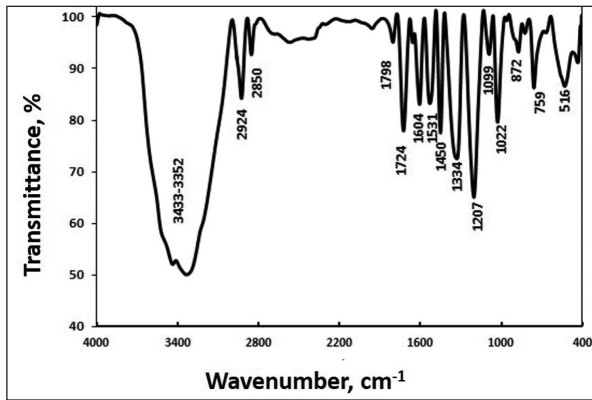


Figure 2. FTIR spectrum of *P. vera* aqueous leaves extract.

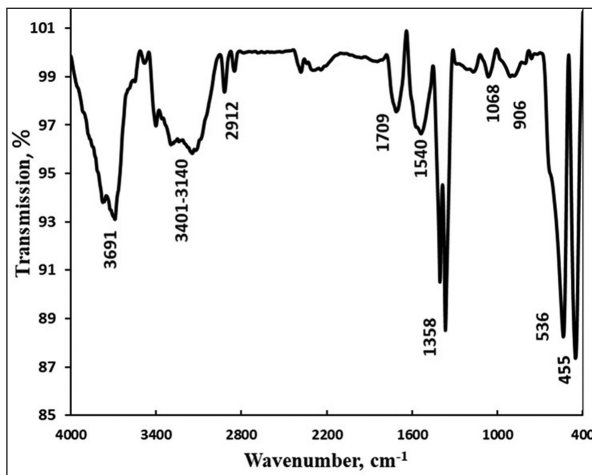


Figure 3. FT-IR spectrum of the synthesized hematite ($\alpha\text{-Fe}_2\text{O}_3$) nanoparticles, heated at 550°C for 2h.

3.2 X-ray Diffraction (XRD) Analysis

The X-ray diffraction (XRD) verifies the crystalline configuration of synthesized $\alpha\text{-Fe}_2\text{O}_3$ nanoparticles. The diffractogram in Figure 4 demonstrates the sharp peaks at twenty degree values 23.92°, 32.96°, 35.48°, 40.54°, 49.31°, 53.91°, 62.12°, and 63.76°. The exhibited peaks corresponded to 012, 104, 110, 113, 024, 116, 214, and 300 plans, respectively. The diffraction peaks are well-matched with Joint Committee on Powder Diffraction Standards (JCPDS) card no. 33-0664, endorsing that the $\alpha\text{-Fe}_2\text{O}_3$ nanoparticles have a hexagonal crystalline configuration. Moreover, no further diffraction peaks of other stages are detected, which signifies the high purity level of the $\alpha\text{-Fe}_2\text{O}_3$ nanoparticles. The average crystallite size of the synthesized nanoparticles is 40 nm.

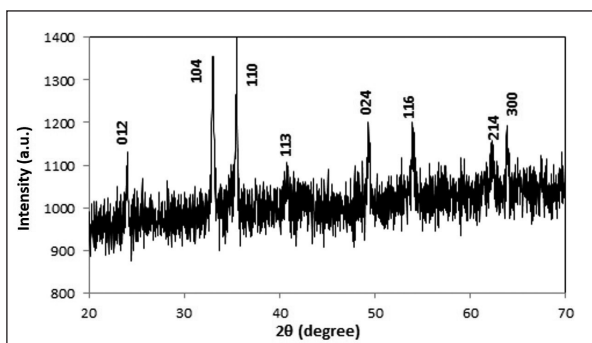


Figure 4. XRD pattern of the synthesized hematite ($\alpha\text{-Fe}_2\text{O}_3$) nanoparticles.

3.3 UV-vis Spectroscopy Analysis

UV-visible spectroscopy is a spectral technique used to certify the formation and constancy of metal nanoparticles in aqueous solutions. Figure 5 shows that the UV-visible absorption of the $\alpha\text{-Fe}_2\text{O}_3$ nanoparticles was the maximum in the wavelength range of 460-480 nm. The SPR bands of the colloidal iron nanoparticles were centered at around 480 nm for the $\alpha\text{-Fe}_2\text{O}_3$ nanoparticles prepared by the green method (Figure 5). The reaction mixtures showed a single surface plasmon resonance (SPR) band; this demonstrates the spherical shape of the hematite nanoparticles, which was further confirmed by TEM images.

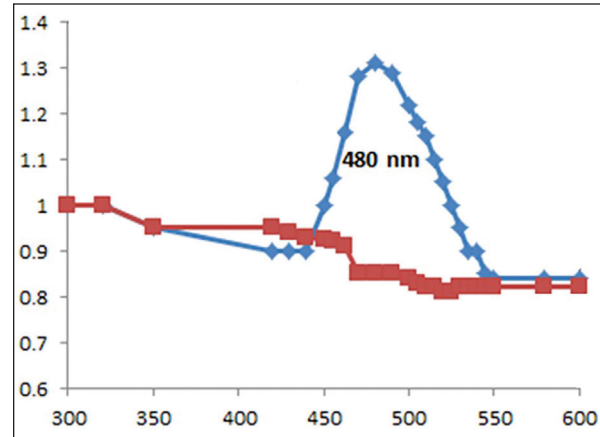


Figure 5. UV- vis absorption spectra of $\alpha\text{-Fe}_2\text{O}_3$ (blue line) and *P. vera* leaves extract (red line).

3.4 TEM Analysis

The hematite ($\alpha\text{-Fe}_2\text{O}_3$) nanoparticles are composed of invariable nanoparticles of a nearly spherical morphology with a narrow-size distribution (Figure 6). The nanoparticles size was in the range of 40 nm. It was very dependent on the type and concentration of the utilized base in the preparation process of hematite. However, a direct correlation governs the relationship between the base concentration and the resulted nanoparticle. This correlation was noticed by Lassoud et al. (2017).

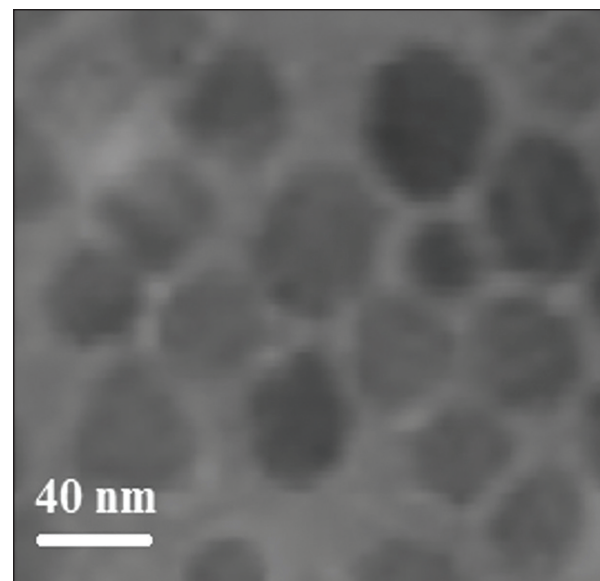


Figure 6. TEM micrograph of synthesized hematite $\alpha\text{-Fe}_2\text{O}_3$ nanoparticles.

3.5 Seed Germination

The effect of the hematite nanoparticle concentrations on the germination percentage (G %), germination rate (GR), and vigor index (VI) of tomato seeds is shown in table 1. In the current study, priming tomato seeds before germination with hematite nanoparticles exhibited a higher vigor index across all treatments (10 to 200 ppm). At the 10 ppm treatment, the germination vigor index has improved by 24 % compared to the control. Seed vigor index is a key indicator of rapid germination and seedling establishment (Barpete et al., 2015). The uppermost vigor index level is linked with the superiority of the tomato plant (Var. newton) to perform more applicably at different concentrations of the $\alpha\text{-Fe}_2\text{O}_3$ nanoparticles (10, 40 and 80 ppm). On the other hand, at higher concentrations (100 and 200 ppm), the seed vigor index had a negative impact on seed vigor compared to a lower concentration of the $\alpha\text{-Fe}_2\text{O}_3$ nanoparticles (10 ppm). This may be attributed to the

toxicity degree caused by higher concentrations as reported by Shankamma et al., (2016). Another explanation could be the status of the massing and clustering of nanoparticles in high concentrations which leads to block the nanoholes and reduce element uptake (Ren et al., 2011).

The application of $\alpha\text{-Fe}_2\text{O}_3$ nanoparticles significantly increased seedling growth parameters (shoot length, seedling fresh and dry weights) compared to the control ($p < 0.001$, $p < 0.005$ and $p < 0.01$; respectively) (Table 2). Interestingly, the response of tomato seeds to a lower concentration (10 ppm) recorded better or similar results compared to high concentrations. At 10 ppm, the shoot length increased by 48.6 %, the seedling fresh weight by 41 %, and the dry weight by 135 % compared to the control. Overall, it is believed in this study that a low concentration (10 ppm) of $\alpha\text{-Fe}_2\text{O}_3$ is adequate to induce vigor index and growth parameters in 'Newton' tomatoes.

Table 2. Effect of seed treatment with various hematite (FeNPs) concentrations on tomato seedling growth parameters. Different letters indicate statistically-significant differences among treatments ($P < 0.05$). NS not significant.

FeNPs (ppm)	Shoot length (cm)	Root length (cm)	Seedling fresh weight (g)	Seedling dry weight (g)
Control	3.62 d	7.47	0.17 c	0.017 b
10	5.38 a	7.11	0.24 ab	0.040 a
40	4.70 c	7.60	0.20 bc	0.037 a
80	4.74 bc	6.83	0.23 ab	0.040 a
100	4.93 bc	5.98	0.26 a	0.037 a
200	5.00 b	6.53	0.22 b	0.040 a
<i>P value</i>	<i><.001</i>	<i>NS</i>	<i>0.005</i>	<i>0.01</i>

Although the biological indicators of phytotoxicity were not investigated in this study, the negative responses of seed germination, root and shoot length parameters to high $\alpha\text{-Fe}_2\text{O}_3$ levels (e.g. 100 and 200 ppm) support the hypothesis that a high concentration of $\alpha\text{-Fe}_2\text{O}_3$ can lead to phyto-toxicity (Kumar et al., 2015). In fact, Phyto-toxicity can lead to the reduction of germination and negative modifications of plant growth and oxidative-stress resistance (Chen et al., 2010; Rajeshwari et al., 2015). In this study, no negative impacts were detected on germination indices, and shoot and root length, which indicates that hematite ($\alpha\text{-Fe}_2\text{O}_3$) nanoparticles (10 ppm, 40 ppm, 80 ppm, 100 ppm and 200 ppm) are not phytotoxic to the 'Newton' tomato seeds.

4. Conclusion

In this work, hematite ($\alpha\text{-Fe}_2\text{O}_3$) nanoparticles were efficaciously prepared from *P. vera* leaves by an innovative green technique. Iron nitrate nonahydrate ions were utilized as a precursor and of the *P. vera* leaf aqueous extract as a stabilizing and capping agent. FTIR confirms the presence of Fe-O stretching vibration. The obtained results indicate that the synthesized hematite nanoparticles are spherically-shaped and are 40 nm in size. A low concentration of hematite ($\alpha\text{-Fe}_2\text{O}_3$) nanoparticles (10 ppm) was adequate to promote seed vigor index and growth parameters compared to other higher concentrations. The current results confirm the promising potential of hematite ($\alpha\text{-Fe}_2\text{O}_3$) nanoparticles to be utilized in seed priming and agricultural production.

Acknowledgments

The authors are thankful to the Deanship of Scientific Research, at the University of Jordan, in Amman, Jordan and to the Royal Scientific Society for providing all the facilities and support to carry out this research.

References

- Ahmmad, B., Leonard, K., Islam M.S., Kurawaki, J.; Muruganandham, M., Ohkubo, T., Kuroda, Y. (2013). Green synthesis of mesoporous hematite ($\alpha\text{-Fe}_2\text{O}_3$) nanoparticles and their photocatalytic activity. *Advanced Powder Technology*, 24(1): 160-167.
- Ali, H.R., Nassar, H.N., El-Gendy, N.S. (2017). Green synthesis of $\alpha\text{-Fe}_2\text{O}_3$ using Citrus reticulatum peels extract and water decontamination from different organic pollutants. *J. Energy Sour., Part A: Recovery, Util. Environ. Effects*, 39: 1425-1434.
- Asoufi, H.M., Al-Antary, T.M., Awwad, A.M. (2018). Green route for synthesis hematite ($\alpha\text{-Fe}_2\text{O}_3$) nanoparticles: Toxicity effect on the green peach aphid, *Myzus persicae* (Sulzer). *Environmental Nanotechnology, Monitoring & Management*, 9: 107-111.
- Awwad, A.M., and Salem, N.M. (2012). Green synthesis of silver nanoparticles by mulberry leaves extract. *Nanoscience and Nanotechnology*, 2(4): 125-128.
- Ayad, J.Y., Al-Abdallat, A.M., Saoub, H.M. (2010). Growth and yield of spring wheat and barley genotypes. *International Journal of Botany*, 6(4): 404-413.
- Badni, N., Benheraoua, F.Z., Tadjer, B., Boudjemaa, A., El Hameur, H., Bachari, K. (2016). Green synthesis of $\alpha\text{-Fe}_2\text{O}_3$ nanoparticles using Roman nettle. *Third International Conference on Energy, Materials, Applied Energetics and Pollution ICEMAEP2016*, October 30-31, 2016 (Constantine, Algeria).

- Barpete, S., Oğuz, M.C., Özcan, S.F., Anayol, E., Ahmed, H.A., Khawar, K.M., Özcan, S. (2015). Effect of temperature on germination, seed vigor index and seedling growth of five Turkish cotton (*Gossypium hirsutum* L.) cultivars. *Fresenius Environ Bull*, 24: 1-7.
- Basavegowda, N., Mishra, K., Lee, Y.R. (2017). Synthesis, characterization, and catalytic applications of hematite (α -Fe₂O₃) nanoparticles as reusable nanocatalyst. *Advances in Natural Sciences, Nanoscience and Nanotechnology*, 8(2): 025017.
- Chen, R., Ratnikov, T.A., Stone, M.B., Lin, S., Lard, M., Huang, G., Hudson, J.S., Ke, P.C. (2010). Differential Uptake of Carbon Nanoparticles by Plant and Mammalian Cells. *Small* 6: 612–617. <http://dx.doi.org/10.1002/sml.200901911>
- Dong, C.D., Chen, C.W., Hung, C.M. (2016). Magnetic nanoparticles and their heterogeneous persulfate oxidation organic compound applications. In *Advanced Materials* (pp. 23-35). Springer, Cham
- Groiss, S., Selvaraj, R., Varadavenkatesan, T., Vinayagam, R. (2017). Structural characterization, antibacterial and catalytic effect of iron-oxide nanoparticles synthesised using the leaf extract of *Cynometra ramiflora*. *Journal of Molecular Structure*, 1128: 572-578.
- Hoag, G.E., Collins, J.B., Holcomb, J.L., Hoag, J.R., Nadagouda, M.N., Varma, R.S. (2009). Degradation of bromothymol blue by 'greener' nano-scale zero-valent iron synthesized using tea polyphenols. *Journal of Materials Chemistry*, 19(45): 8671-8677.
- International Seed Testing Association (ISTA). *International Rules for Seed Testing*. (2008). Bassersdorf, CH. Switzerland.
- Jagathesan, G., and Rajiv, P. (2018). Biosynthesis and characterization of iron-oxide nanoparticles using *Eichhornia crassipes* leaf extract and assessing their antibacterial activity. *Biocatalysis and agricultural biotechnology*, 13: 90-94.
- Jain, T.K., Morales, M.A., Sahoo, S.K., Leslie-Pelecky, D.L., Labhasetwar, V. (2005). Iron oxide nanoparticles for sustained delivery of anticancer agents. *Molecular pharmaceutics*, 2(3): 194-205.
- Kolen'ko, Y.V., Bañobre-López, M., Rodríguez-Abreu, C., Carbó-Argibay, E., Sailsman, A., Piñeiro-Redondo, Y., Rivas, J. (2014). Large-scale synthesis of colloidal Fe₃O₄ nanoparticles exhibiting high heating efficiency in magnetic hyperthermia. *The Journal of Physical Chemistry C*, 118(16): 8691-8701.
- Kumar, S., Patra, A.K., Datta, S.C., Rosin, K.G., Purakayastha, T.J. (2015). Phytotoxicity of nanoparticles to seed germination of plants. *International Journal of Advanced Research*, 3(3): 854-865.
- Lassoued, A., Lassoued, M.S., Dkhil, B., Gadri, A., Ammar, S. (2017). Synthesis, structural, optical and morphological characterization of hematite through the precipitation method, Effect of varying the nature of the base. *Journal of Molecular Structure* 1141: 99-106.
- Li, J., Hu, J., Ma, C., Wang, Y., Wu, C., Huang, J., Xing, B. (2016). Uptake, translocation and physiological effects of magnetic iron oxide (γ -Fe₂O₃) nanoparticles in corn (*Zea mays* L.). *Chemosphere*, 159: 326-334.
- Madhavi, V., Prasad, T.N.V.K.V., Reddy, A.V.B., Reddy, B.R., Madhavi, G. (2013). Application of phytogenic zerovalent iron nanoparticles in the adsorption of hexavalent chromium. *Spectrochimica Acta Part A, Molecular and Biomolecular Spectroscopy*, 116: 17-25.
- Nadagouda, M.N., Hoag, G., Collins, J., Varma, R.S. (2009). Green synthesis of Au nanostructures at room temperature using biodegradable plant surfactants. *Crystal Growth & Design*, 9(11): 4979-4983
- Pariona, N., Martinez, A.I., Hdz-García, H.M., Cruz, L.A., Hernandez-Valdes, A. (2017). Effects of hematite and ferrihydrite nanoparticles on germination and growth of maize seedlings. *Saudi journal of biological sciences*, 24(7): 1547-1554
- Parsons, J.G., Peralta-Videa, J.R., Gardea-Torresdey, J.L. (2007). Use of plants in biotechnology, synthesis of metal nanoparticles by inactivated plant tissues, plant extracts, and living plants. *Developments in environmental science*, 5: 463-485.
- Rajeshwari, A., Kavitha, S., Alex, S.A., Kumar, D., Mukherjee, A., Chandrasekaran, N., Mukherjee, A. (2015). Cytotoxicity of aluminum oxide nanoparticles on *Allium cepa* root tip—effects of oxidative stress generation and biouptake. *Environ. Sci. Pollut. Res.*, 22: 11057–11066. <http://dx.doi.org/10.1007/s11356-015-4355-4>.
- Ramimoghdam, D., Bagheri, S., Hamid, S.B.A. (2014). Progress in electrochemical synthesis of magnetic iron oxide nanoparticles. *J. Magn. Magn. Mater.* 368: 207–229.
- Ren, G., Yang, L., Zhang, Z., Zhong, B., Yang, X., Wang, X. (2017). A new green synthesis of porous magnetite nanoparticles from waste ferrous sulfate by solid-phase reduction reaction. *Journal of Alloys and Compounds*, 710: 875-879
- Ren, H. X., Liu, L., Liu, C., He, S.Y., Huang, J., Li, J.L., Gu, N. (2011). Physiological investigation of magnetic iron oxide nanoparticles towards chinese mung bean. *Journal of biomedical nanotechnology*, 7(5): 677-684.
- Seabra, A.B., Haddad, P., Duran, N. (2013). Biogenic synthesis of nanostructured iron compounds, applications and perspectives. *IET nanobiotechnology*, 7(3): 90-99.
- Salem, N.M., Ahmad, A.L., Awwad, A.M. (2013). New route for synthesis magnetite nanoparticles from ferrous ions and pistachio leaf extract. *Nanoscience and Nanotechnology*, 3(3): 48-51.
- Shameli, K., Bin Ahmad, M., Jazayeri, S.D., Sedaghat, S., Shabanzadeh, P., Jahangirian, H., Abdollahi, Y. (2012). Synthesis and characterization of polyethylene glycol mediated silver nanoparticles by the green method. *International journal of molecular sciences*, 13(6): 6639-6650.
- Shankramma, K., Yallappa, S., Shivanna, M.B., Manjanna, J. (2016). Fe₂O₃ magnetic nanoparticles to enhance *S. lycopersicum* (tomato) plant growth and their biomineralization. *Applied Nanoscience*, 6(7): 983-990.